Accumulation and purging of deleterious mutations through severe bottlenecks in ibex

Christine Grossen[1,*], Frederic Guillaume[1], Lukas F. Keller[1,2,a,*], Daniel Croll[3,a,*]

[1]Department of Evolutionary Biology and Environmental Studies, University of Zurich, Zurich, Switzerland

[2]Zoological Museum, University of Zurich, Karl-Schmid-Strasse 4, Zurich, Switzerland

[3]Laboratory of Evolutionary Genetics, Institute of Biology, University of Neuchâtel, Neuchâtel, Switzerland

[a] LFK and DC contributed equally to this work

[*]Authors for correspondence: christine.grossen@ieu.uzh.ch, lukas.keller@ieu.uzh.ch, daniel.croll@unine.ch

Author contributions:

Conception and design of study: CG, DC, LFK

Acquisition and analysis of data: CG

Interpretation of data: CG, DC, LFK, FG

Funding: CG, LFK

Wrote the manuscript with input from the other authors: CG, DC

Abstract

Population bottlenecks have a profound impact on the genetic makeup of a species including levels of deleterious variation. How reduced selection efficacy and purging interact is known from theory but largely lacks empirical support. Here, we analyze patterns of genome-wide variation in 60 genomes of six ibex species and the domestic goat. Ibex species that suffered recent severe bottlenecks accumulated deleterious mutations compared to other species. Then, we take advantage of exceptionally well-characterized repeated bottlenecks during the restoration of the near-extinct Alpine ibex and show that experienced bottleneck strength correlates with elevated individual inbreeding. Strong bottlenecks led to the accumulation of mildly deleterious mutations and purging of highly deleterious mutations. We show in a simulation model that realistic bottleneck strengths can indeed simultaneously purge highly deleterious mutations during overall mutation accumulation. Genome-wide purging of highly deleterious mutation load over few generations in the wild has implications for species conservation efforts.

Main text

Dramatic, temporary reductions in population size – so-called bottlenecks – occur in nearly all plant and animal populations including humans [1]. These demographic changes have important consequences for wildlife management and the conservation of endangered species [2], but they also have profound consequences including genetic disorders [e.g 3-7]. Increased genetic drift and inbreeding due to bottlenecks lead to loss of neutral genetic variation, a reduced efficacy of natural selection, and increased expression of deleterious recessive mutations [8-10]. The expression of recessive mutations under inbreeding creates the potential for selection to act against these mutations, a process known as purging. Purging reduces the frequency of deleterious mutations depending on the population size, the degree of dominance, and the magnitude of the deleterious effects [11]. Unless population sizes are extremely low, bottlenecks tend to purge highly deleterious, recessive mutations [11,12]. On the other hand, genetic drift during bottlenecks reduces the efficacy of selection [13]. This allows mildly deleterious mutations to drift to substantially

51 higher frequencies [6,14]. The combination of purging and reduced selection efficacy generates complex
52 dynamics of deleterious mutation frequencies following population bottlenecks [11,12,15-17].
53
54 Theory predicts how reduced selection efficacy and purging impact the mutation load through
55 bottlenecks [11,15,16,18], but genetic evidence from wild populations is rare [19-21]. Most previous research
56 used changes in fitness to infer possible purging events [18,21-24], but changes in fitness can result from
57 causes unrelated to purging such as adaptation to specific environmental conditions or the fixation of
58 deleterious mutations [10,25]. One study provided direct evidence for purging of the most deleterious
59 mutations in isolated mountain gorilla populations that split off larger lowland populations ~20'000
60 years ago [19]. However, it remains unknown how more complex or recent demographic events affect
61 levels of deleterious mutations in the wild. Here, we take advantage of exceptionally well characterized
62 repeated bottlenecks during the reintroduction of the near-extinct Alpine ibex to retrace the fate of
63 deleterious mutations. Alpine ibex were reduced to ~100 individuals in the 19th century in a single
64 population in the Gran Paradiso region of Northern Italy [26]. In less than a century, a census size of ca.
65 50'000 individuals has been re-established across the Alps. Thus, the population bottleneck of Alpine
66 ibex is among the most dramatic recorded for any successfully restored species. Most extant populations
67 experienced at least three bottlenecks leaving strong footprints of low genetic diversity [27,28].
68

Figure 1

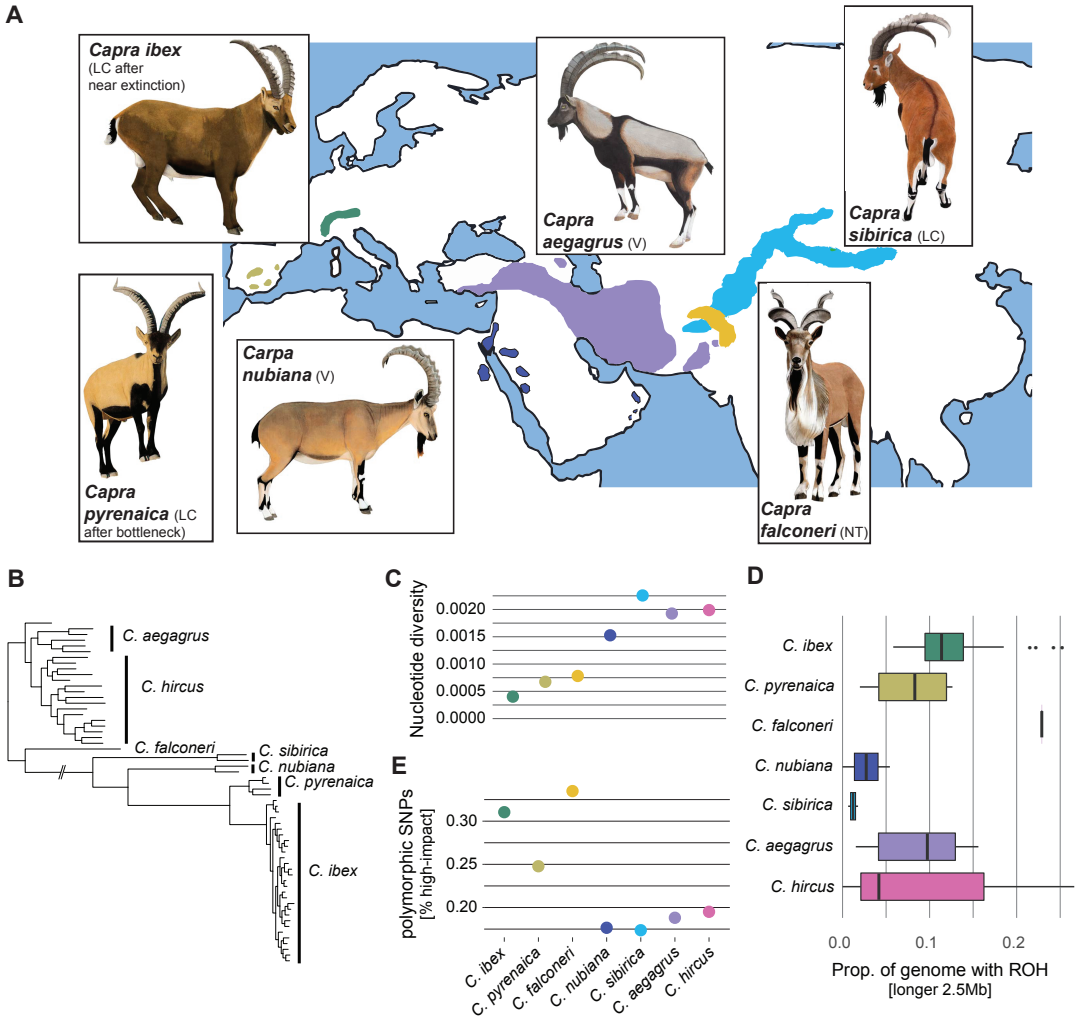

Figure 1: Characterization of sampled ibex species. A) Geographical distribution and IUCN conservation status of ibex and wild goat species (LC: Least concern, V: Vulnerable, NT: Near threatened [60]). Sample izes: *C. ibex*: N=29, *C. pyrenaica*: N=4, *C. aegagrus*: N=6, *C. sibirica*: N=2, *C. falconeri*: N=1, *C. nubiana*: N=2. B) Maximum likelihood phylogenetic analyses, C) nucleotide diversity, D) proportion of the genome with runs of homozygosity (ROH) longer than 2.5 Mb and E) percentage of polymorphic sites within species that segregate highly deleterious mutations.

We analyze 60 *Capra* genomes covering Alpine ibex (*C. ibex*), five additional wild goats and the domestic goat, we find exceptionally low genome-wide variation and an accumulation of deleterious mutations in Alpine ibex (Figure 1). Both nucleotide diversity and number of heterozygous sites per kb sequenced was lowest in Alpine ibex and Iberian ibex (*C. pyrenaica*), the two species that experienced the strongest recent bottlenecks (Figure 1C, Figure S2, Tables S1 and S2). Genome-wide diversity was highest in Siberian ibex (*C. sibirica*), which have large and relatively well-connected populations [29].

Genomes of the Siberian and Nubian ibex (*C. nubiana*) and of some domestic goat (*C. aegagrus hircus*) showed the least evidence for recent inbreeding estimated by genome-wide runs of homozygosity (ROH) [30]. In contrast, the genomes of some Alpine ibex, the Markhor (*C. falconeri*), and some domestic goat individuals contained more than 20% ROH (Figure 1D, Figures S3A and B, Table S3). Overall, there was clear genomic evidence that the near extinction and recovery of the Alpine ibex resulted in substantial genetic drift and inbreeding, opening the possibility for purging and accumulation of deleterious mutations.

We analyzed all *Capra* genomes for evidence of segregating deleterious mutations (Figure S6). We restricted our analyses to autosomal coding sequences with evidence for transcriptional activity in Alpine ibex organs. We further removed sites with low genomic evolutionary rate profiling (GERP) [31] scores yielding a total of 370'853 SNPs (Table S4). We functionally annotated SNP variants for the expected impact on the protein function. We found that across all seven *Capra* species 0.17% of these SNPs carried a highly deleterious variant with the majority incurring a stop-gain mutation (Table S4). We found that the proportion of highly deleterious mutations varied substantially among *Capra* species (Figure 1E, Figures S7A to D). The proportion of highly deleterious variants segregating within species was inversely correlated with nucleotide diversity (Pearson, df=5, r=-0.86, p=0.012). Hence, the *Capra* species with the smallest populations or the most severe population size reductions show an accumulation of deleterious mutations.

Both Alpine and Iberian ibex experienced severe bottlenecks due to overhunting and habitat fragmentation. Historic records indicate that Alpine ibex suffered a bottleneck of ~100 individuals at the end of the 19th century and Iberian ibex a bottleneck of ~1000 individuals [32] (Table S1). We first looked for evidence of purging in the allele frequency spectra of mutation classes of varying severity. We focused only on derived sites that were polymorphic in at least one of the two sister species (Figure 2A, S8). We found that frequency distributions of high and moderate impact mutations in Alpine ibex were downwards shifted indicating purifying selection (Figure 2C and GERP score analyses in Figure S9A). Short indels (≤ 10 bp) in coding sequences revealed a similar shift towards lower frequencies

(Figure S9B). This is consistent with stronger selection acting against highly deleterious mutations in Alpine ibex.

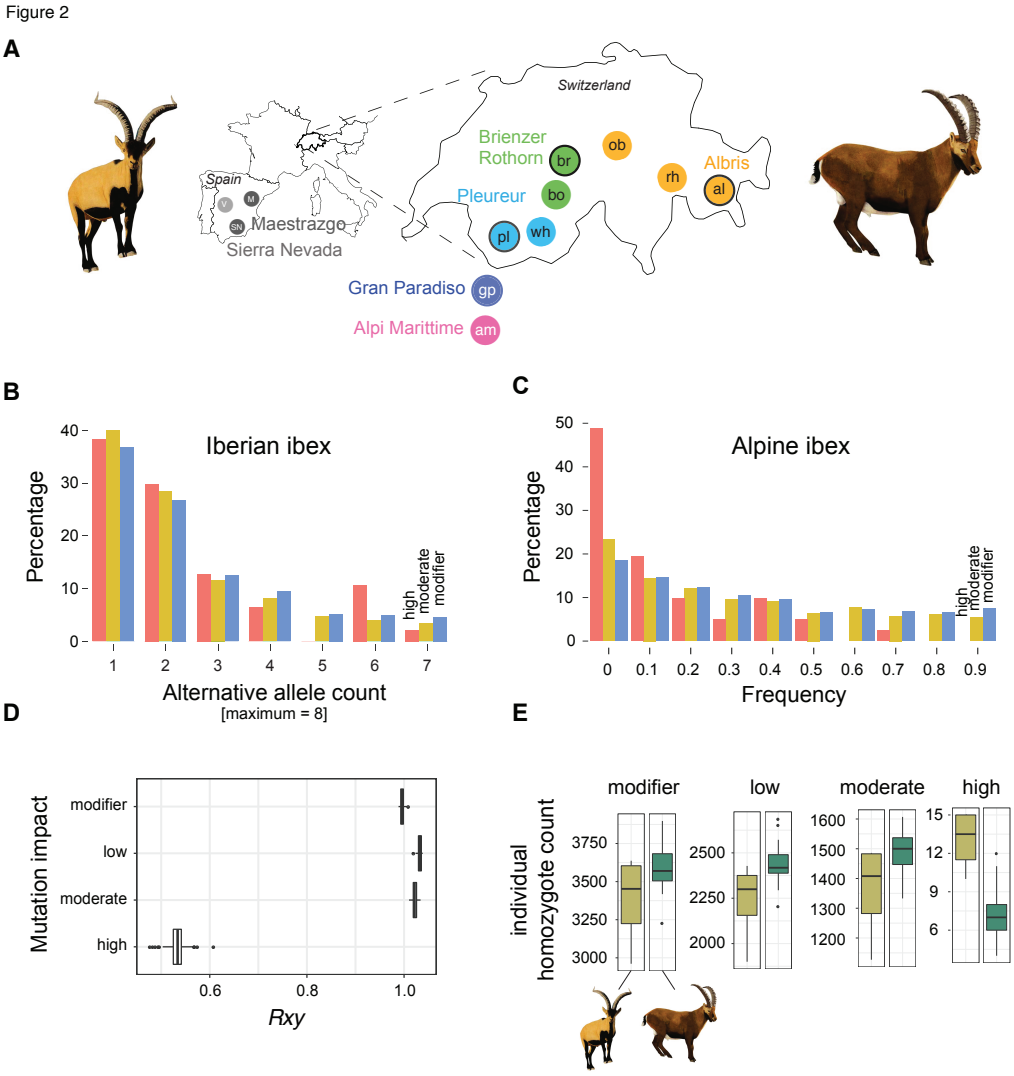

Figure 2: Segregating deleterious mutations in Alpine and Iberian ibex. A) Population sampling locations of Iberian ibex (left, grey circles) and Alpine ibex (right, colored circles). Each filled circle represents a population. Circles with a black outline indicate the first three reintroduced populations in Switzerland that were used for all subsequent population reintroductions of Alpine ibex. Colors associate founder and descendant populations (see also Figure 3A). Site frequency spectra for neutral (modifier), mildly (moderate impact) and highly deleterious (high impact) mutations for (B) Iberian and (C) Alpine ibex. D) *Rxy* analysis contrasting Iberian with Alpine ibex across the spectrum of impact categories. *Rxy* < 1 indicates a relative frequency deficit of the corresponding category in Alpine ibex compared to Iberian ibex. E) Individual homozygote counts per impact category for Iberian (light green) and Alpine ibex (dark green).

To test whether Alpine ibex indeed showed evidence for purging of deleterious mutations compared to Iberian ibex, we calculated the relative number of derived alleles *Rxy* [33] for each mutation impact category (Figure 2D). We used a random set of intergenic SNPs for standardization, which makes *Rxy* robust against sampling effects and population substructure [33]. Low and moderate impact mutations (*i.e.* mildly deleterious mutations) showed a minor excess in Alpine ibex compared to Iberian ibex, indicating a higher load in Alpine ibex. In contrast, we found that highly deleterious mutations were strongly reduced in Alpine ibex compared to Iberian ibex (Figure 2D). Strikingly, the proportion of SNPs across the genome segregating a highly deleterious mutation is higher in Alpine ibex (Figure 1E), but *Rxy* shows that highly deleterious mutations have a pronounced downwards allele frequency shift in Alpine ibex compared to Iberian ibex (Figure 2C). Furthermore, the number of homozygous sites with highly deleterious mutations per individual were considerably lower in Alpine ibex than Iberian ibex (Figure 2E). Together, this shows that highly deleterious mutations were substantially purged in Alpine ibex. We also found evidence for the accumulation of mildly deleterious mutations through genetic drift in Alpine ibex.

Consistent with the fact that all extant Alpine ibex originate from the Gran Paradiso, this population occupies the center of a principal component analysis (Figure 3A-B, Figure S11A-B; [28]). The first populations re-established in the Alps were already clearly distinct from the Gran Paradiso source population and showed reduced nucleotide diversity (Figure 3A, C), having experienced 1 or 2 additional bottlenecks [27]. These initial three reintroduced populations were used to establish additional populations, which underwent a total of 3-4 bottlenecks. These additional bottlenecks lead to further loss of nucleotide diversity and genetic drift, as indicated by the increasing spread in the principal component analysis (Figure 3A-C). An exceptional case constitutes the Alpi Marittime population, which was established through the translocation of 25 Gran Paradiso individuals of which only six successfully reproduced [34]. As expected from such an extreme bottleneck, Alpi Marittime showed strong genetic differentiation from all other Alpine ibex populations and highly reduced nucleotide diversity (Figures 3B-C; [35]). To estimate the expected strength of drift experienced by different populations, we estimated effective population sizes through the long-term harmonic mean population

sizes based on demographic records spanning the near century since establishment [36,37]. We found that both the nucleotide diversity and the individual number of heterozygous sites per kb decreased with smaller long-term population size (Figure 3C, Figure S12). In parallel to genetic drift, inbreeding was also higher in the populations with the lowest harmonic mean population sizes. Genomes from the Gran Paradiso source population generally showed the lowest proportions of the genome affected by ROH, while reintroduced populations of lowest effective population size had the highest proportions of the genome affected by ROH (Figure 3D and Figure S3).

Figure 3

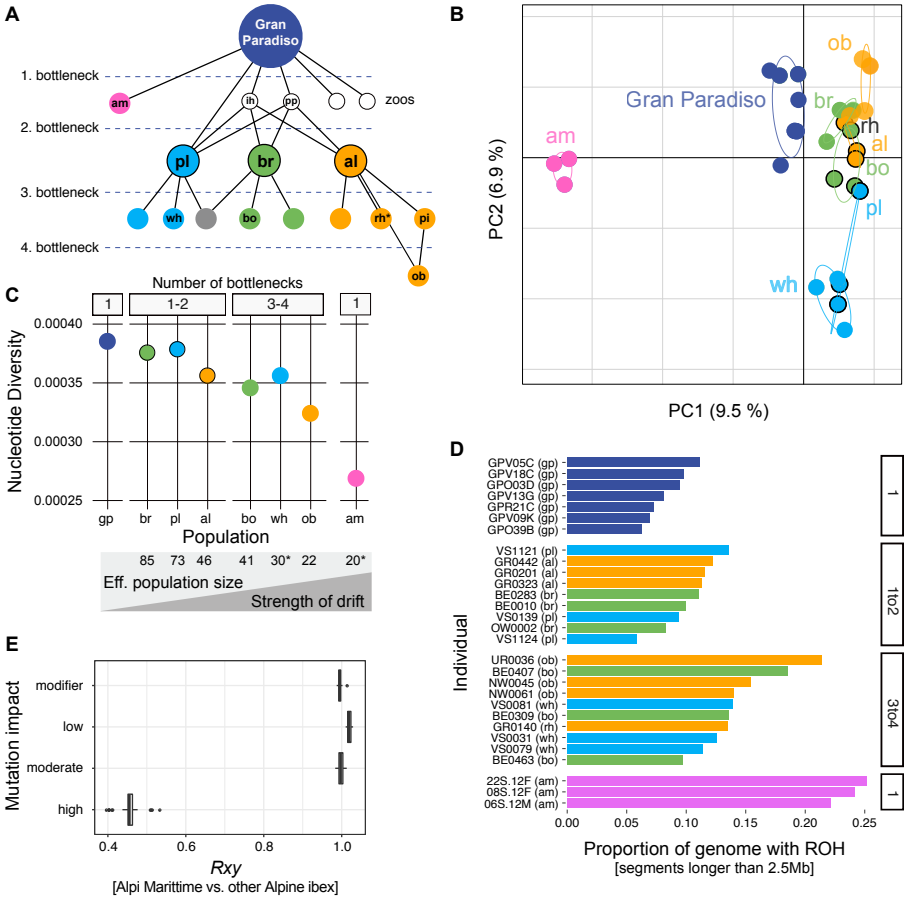

Figure 3: Population genomic consequences of Alpine ibex recolonization. A) Schematic showing the recolonization history and population pedigree of Alpine ibex. Locations include also zoos and the population Pilatus (pi), which was not sampled for this study but is known to have contributed to the population Oberbauenstock (ob). am: Alpi Marittime, gp: Gran Paradiso; ih: Zoo Interlaken Harder; al: Albris; bo: Bire Öschinen; br: Brienzer Rothorn; ob: Oberbauenstock; pl: Pleureur; rh: Rheinwald; wh: Weisshorn; pi: Pilatus; pp: Wildpark Peter and Paul. The grey circle represents a population that was founded from more than one population. Figure elements were modified from Biebach and Keller (2009) with permission. B) Principal component analysis of all Alpine ibex individuals included in the study. C) Nucleotide diversity per population. D) Proportion of the genome within runs of homozygosity (ROH) longer than 2.5 Mb. E) *Rxy* analysis contrasting the strongly bottlenecked Alpi Marittime population with all other Alpine ibex populations across the spectrum of impact categories. *Rxy* < 1 indicates a relative frequency deficit of the corresponding category in the Alpi Marittime population. Circles with a black outline indicate the first three reintroduced populations in Switzerland that were

used for all subsequent population reintroductions of Alpine ibex. Colors associate founder and descendant populations.

Bottlenecks should affect deleterious mutations by randomly increasing or decreasing allele frequencies at individual loci. As predicted from theory, we find that individuals from populations that underwent stronger bottlenecks carry significantly more homozygotes for modifier, low and moderate impact mutations (*i.e.* nearly neutral and mildly deleterious mutations; Figure 4A). In contrast, individuals showed no meaningful difference in number of homozygotes for high impact (*i.e.* highly deleterious) mutations across populations. The stability in the number of homozygotes for high impact mutations through successive bottlenecks despite a step-wise increase in the number of homozygotes for weaker impact mutations, strongly suggests that purging occurred over the course of the Alpine ibex reintroductions. This finding was confirmed using an alternative categorization of deleterious mutation load based on phylogenetic conservation based GERP scores (Figure S13). Because the above findings are contingent on a model where deleterious mutations are recessive, we also analyzed the total number of derived alleles per individual. We find a consistent but less pronounced increase in total number of derived alleles per individual for nearly neutral and mildly deleterious mutations (Figure 4B). In contrast, the total number of derived alleles for highly deleterious mutations did not correlate with the strength of bottleneck and was lowest in the most severely bottlenecked Alpi Marittime population (Figure 4B), suggesting that the most deleterious mutations were purged in this population. The *Rxy* statistics showed a corresponding strong deficit in the Alpi Marittime population (Figure 3E). This is consistent with substantially more purging in the most bottlenecked Alpine ibex population.

Figure 4

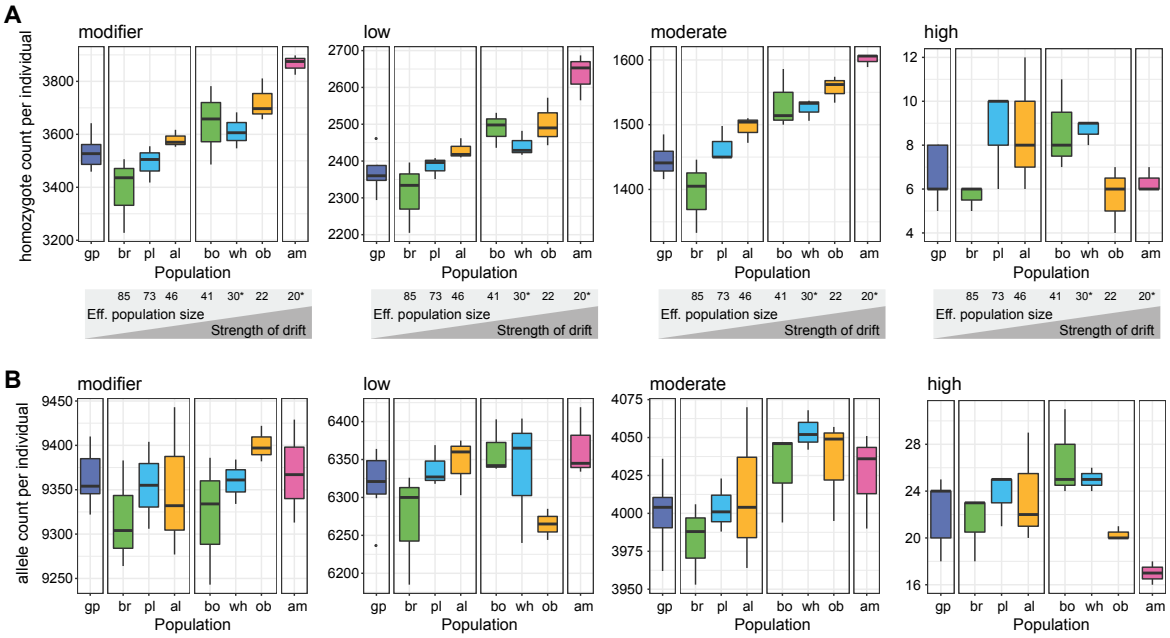

Figure 4: Impact of recolonization on the mutation load per individual. (A) Homozygote counts and (B) allele counts per individual for each Alpine ibex population. The schematic between A and B indicates the harmonic mean of the census size of each population, which is inversely correlated with the strength of drift. *) Estimated numbers. Colors associate founder and descendant populations (see also Figure 3A).

We analyzed the predicted protein truncation by highly deleterious mutations using homology-based inferences. Focusing on high-impact mutations segregating in Alpine ibex, we found that nearly all mutations disrupted conserved protein family (PFAM) domains encoded by the affected genes (Figure 5).

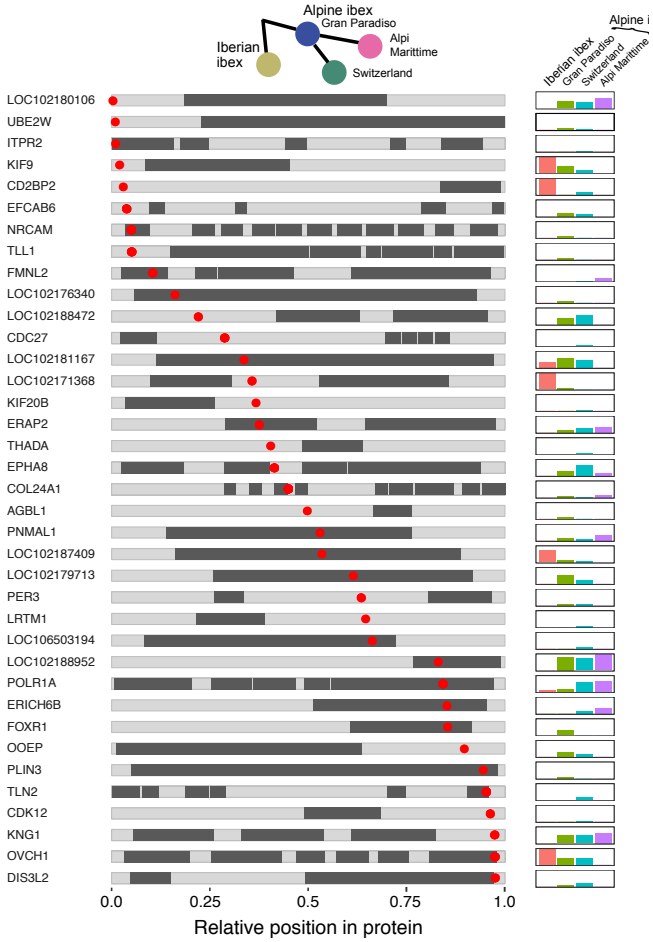

Figure 5: Homology-based inference of the impact of highly deleterious mutations. The localization of protein family (PFAM) domains are highlighted in dark. Red dots indicate the relative position of a highly deleterious mutation segregating in Alpine ibex. The frequencies of highly deleterious mutations are summarized for Iberian ibex and three subsets of Alpine ibex. The demographic history is shown with a schematic.

To ascertain whether accumulation and purging of different mutation classes is indeed expected to occur in the demographic context of the Alpine ibex reintroductions, we parametrized an individual-based forward simulation model with the demographic record[38] (Figure 6A). The model included all populations relevant for the founding of the populations under study and was parametrized with the actual founder size (Figure 6A, S15, Table S1). We used *Rxy* to analyze the evolution of deleterious mutation frequencies through the reintroduction bottlenecks. The simulations showed a deficit of highly deleterious mutations after the reintroduction bottlenecks consistent with purging (Figure 6B). The most bottlenecked Alpi Marittime population also showed evidence of purging of the highly deleterious mutations in the simulated dataset but simultaneously accumulation of mildly deleterious mutations

(Figures 6C, D). Consistent with evidence from *Rxy,* the simulations showed that the number of derived mildly deleterious homozygotes increased with the strength of drift, while no increase was found for highly deleterious mutations (Figure 6D, Figures S17-S20).

Figure 6

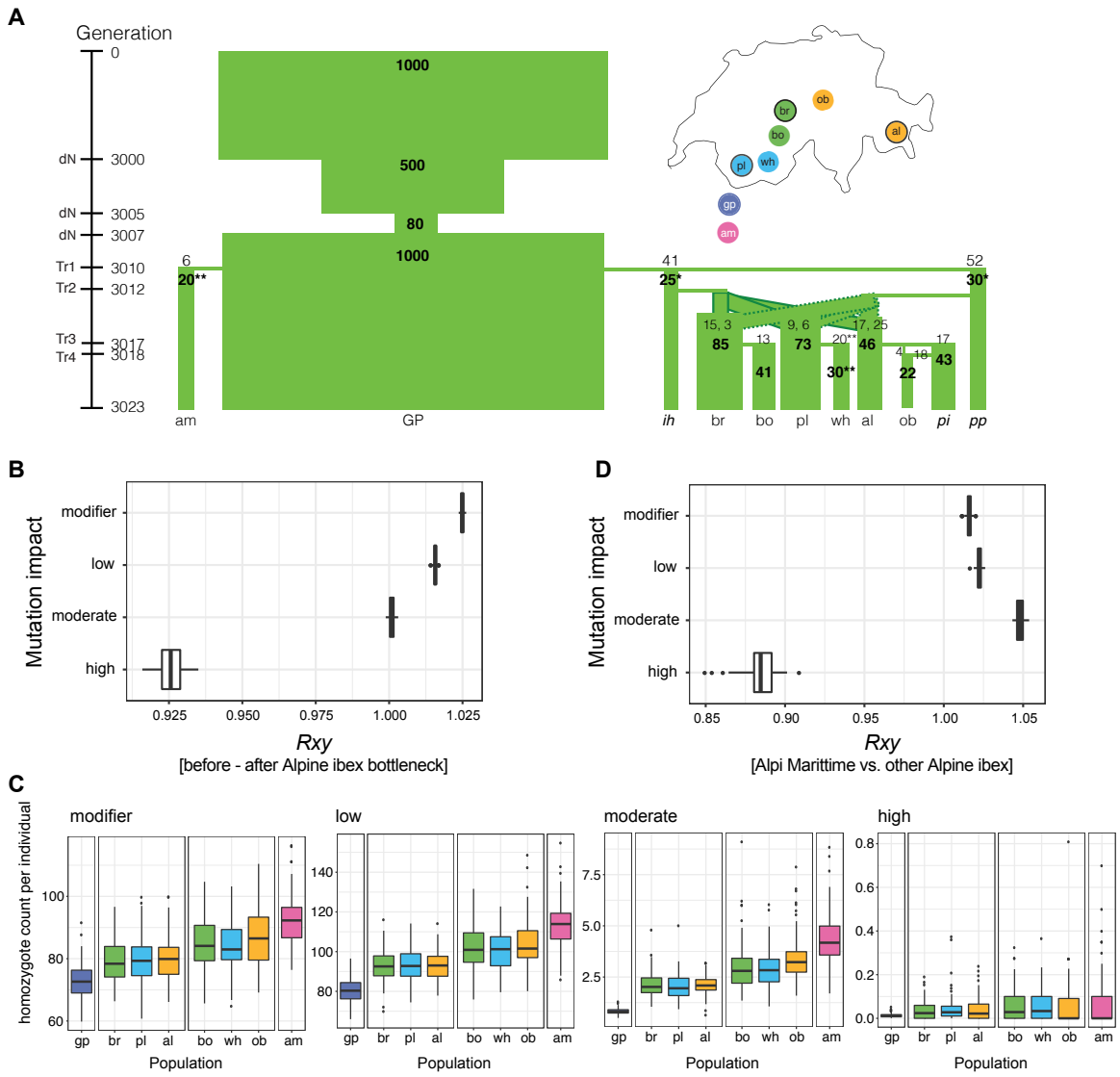

Figure 6: Individual-based forward simulations recapitulating the reintroduction history of Alpine ibex. A) Demographic model used for the individual-based simulations. The model was parametrized using census data and historical records (see methods). Bold numbers represent the carrying capacities defined as the harmonic mean of the census size. Numbers not in bold represent the number of individuals released to found each population. If a population was established from two source populations, the individual numbers are separated by commas. *) Upwards adjusted harmonic means of the census size (historical records were ih=16, Zoo Interlaken Harder, and pp = 20, Wildpark Peter and Paul). The adjustment was necessary to prevent extinction of zoo populations. **) Census numbers were estimated based on historical records of the population but no long- term data census data was available. B) Relative frequency comparison (*Rxy*) of Alpine ibex just before and after the species bottleneck and recolonization. C) *Rxy* analysis contrasting the strongly bottlenecked Alpi Marittime population with all other Alpine ibex populations across the spectrum of impact categories. D) Individual

241 homozygote counts per impact category. Boxplots summarized 100 population means across simulation
242 replicates. Colors associate founder and descendant populations (see also Figure 3A).
243
244
245 Ibex species with recently reduced population sizes accumulated deleterious mutations compared to
246 closely related species. This accumulation was particularly pronounced in the Iberian ibex that
247 experienced a severe bottleneck and Alpine ibex that went nearly extinct. We show that even though
248 Alpine ibex carry an overall higher mutation burden than related species, the strong bottlenecks imposed
249 by the reintroduction of populations purged highly deleterious mutations, the most bottlenecked
250 population (Alpi Marittime) showing the most purging. However, purging was only effective against
251 the most highly deleterious mutations. Empirical evidence for purging in the wild is scarce [18,19]. Here,
252 we show that a few dozen generations were sufficient to reduce the burden of highly deleterious
253 mutations. This suggests that purging may occur widely in populations undergoing severe bottlenecks.
254 It is important to note that mildly deleterious mutations actually accumulated over the course of the
255 reintroduction, consistent with less efficient selection against mildly deleterious mutations in small
256 populations. Hence, the overall mutation load may have increased with bottleneck strength. This is
257 consistent with the finding that population-level inbreeding, which is a strong indicator of past
258 bottlenecks, is correlated with lower population growth rates in Alpine ibex (Bozzuto et al. *in review*).
259 Our empirical results from the Alpine ibex reintroduction are in line with theoretical predictions that
260 populations with an effective size below 100 individuals can accumulate a substantial burden of mildly
261 deleterious mutations within a relatively short time. The burden of deleterious mutations evident in
262 Iberian ibex supports the notion that even population sizes of ~1000 still accumulate mildly deleterious
263 mutations. High loads of deleterious mutations have been shown to increase the extinction risk of a
264 species [39]. Thus, conservation efforts aimed at keeping effective population sizes above a minimum of
265 1000 individuals [2] are well justified.
266

Methods

Genomic data acquisition

DNA samples from 29 Alpine ibex, 4 Iberian ibex, 2 Nubian ibex, 2 Siberian ibex and 1 Markhor individuals were sequenced on an Illumina Hiseq2500 or Hiseq4000 to a depth of 15-38 (median of 17). Table S2 specifies individual sampling locations. Libraries were produced using the TruSeq DNA Nano kit. Illumina sequencing data of 6 Bezoar and 16 domestic goat (coverage 6x – 14x, median 12x) were generated by the NextGen Consortium (https://nextgen.epfl.ch). The corresponding raw data was downloaded from the EBI Short Read Archive: ftp://ftp.sra.ebi.ac.uk/vol1/fastq/.

Read alignment and variant calling

Trimmomatic v.0.36 [40] was used for quality and adapter trimming before reads were mapped to the domestic goat reference genome (version CHIR1, [41]) using Bowtie2 v.2.2.5 [42]. MarkDuplicates from Picard (http://broadinstitute.github.io/picard, v.1.130) was used to mark duplicates. Genotype calling was performed using HaplotypeCaller and GenotypeGVCF (GATK, v.3.6 [43,44]). VariantFiltration of GATK was used to remove single nucleotide polymorphisms (SNP) if: QD <2.0, FS > 40.0, SOR > 5.0, MQ < 20.0, -3.0 > MQRandkSum > 3.0, -3.0 > ReadPosRankSum > 3.0 and AN < 62 (80% of all Alpine ibex individuals). Indels up to 10 bp were also retained and filtered using the same filters and filter parameters, except for not including the filter MQRankSum, because this measure is more likely to be biased for indels of several base pairs. Filtering parameters were chosen based on genome-wide quality statistics distributions (see Figures S21 – S38). Variant positions were independently validated by using the SNP caller Freebayes (v1.0.2-33-gdbb6160 [45]) with the following settings: --no-complex --use-best-n-alleles 6 --min-base-quality 3 --min-mapping-quality 20 --no-population-priors --hwe-priors-off.
To ensure high-quality SNPs, we only retained SNPs that were called and passed filtering using GATK, and that were confirmed by Freebayes. Overall, 97.5 % of all high-quality GATK SNP calls were confirmed by Freebayes. This percentage was slightly lower for chromosome X (96,7%) and unplaced scaffolds (95.2%). We tested whether the independent SNP calls of GATK and Freebayes were concordant and we could validate 99.6% of the biallelic SNPs. We retained genotypes called by GATK.

The total number of SNPs detected was 59.5 million among all species. Per species, the number of SNPs ranged from 21.9 million in the domestic goat (N=16) to 2.0 million in Markhor (N=1, Table S2).

RNA-seq data generation

Tissue samples of a freshly harvested Alpine ibex female were immediately conserved in RNA*later* (QIAGEN) in the field and stored at -80°C until extraction. The following ten organs were sampled: retina/uvea, skin, heart, lung, lymph, bladder, ovary, kidney, liver and spleen. RNA was extracted using the AllPrep DNA/RNA Mini Kit from Qiagen following the manufacturer's protocol. Homogenization of the samples was performed using a Retsch bead beater (Retsch GmbH) in RLT plus buffer (Qiagen). RNA was enriched using a PolyA enrichment protocol implemented in the TruSeq RNA library preparation kit. Illumina sequencing libraries were produced using the Truseq RNA stranded kit. Sequencing was performed on two lanes of an Illumina Hiseq4000.

Genetic diversity and runs of homozygosity

Genetic diversity measured as individual number of heterozygous sites and nucleotide diversity were computed using vcftools [46]. Runs of homozygosity were called using BCFtools/RoH [47], an extension of the software package BCFtools, v.1.3.1. BCFtools/RoH uses a hidden Markov model to detect segments of autozygosity from next generation sequencing data. Due to the lack of a detailed linkage map, we used physical distance as a proxy for recombination rates with the option -M and assuming 1.2cM/Mb following sheep recombination rates [48]. Smaller values for -M led to slightly longer ROH (Figures S3 –S5). Because of small per population sample size, we decided to fix the alternative allele frequency (option --AF-dflt) to 0.4. Estimates for the population with the largest sample size (Gran Paradiso, N=7) were very similar if actual population frequencies (option --AF-estimate sp) were used (Figures S4 and S5). Option --viterbi-training was used to estimate transition probabilities before running the HMM. Running the analysis without the option --viterbi-training led to less but longer ROH (Figures S3-S5).

Identification of high-confidence deleterious mutations

Three lines of evidence were used to identify high-confidence deleterious mutations. First, variants leading to a functional change are candidates for deleterious mutations. We used snpEff [49] v.4.3 for the functional annotation of each variant. The annotation file ref_CHIR_1.0_top_level.gff3 was downloaded from: ftp://ftp.ncbi.nlm.nih.gov/genomes/Capra_hircus/GFF and then converted to gtf using gffread. Option -V was used to discard any mRNAs with CDS having in-frame stop codons. SnpEff predicts the effects of genetic variants (e.g. stop-gain variants) and assesses the expected impact. The following categories were retrieved: high (e.g. stop-gain or frameshift variant), moderate (e.g missense variant, in-frame deletion), low (e.g. synonymous variant) and modifier (e.g. exon variant, downstream gene variant). In the case of overlapping transcripts for the same variant, we used the primary transcript for further analysis. A total of 49.0 % of all detected SNPs were located in intergenic regions, 43.2 % in introns, 6.5 % down- and upstream of genes. A total of 0.7% of variants were within CDS, of which ~60% were synonymous and ~40% were missense variants. Overall, 0.002 % were stop-gain mutations.

Protein sequences were annotated using InterProScan v.5.33 by identifying conserved protein family (PFAM) domains [50].

Second, we assessed the severity of a variant by its phylogenetic conservation score. A non-synonymous variant is more likely to be deleterious if it occurs in a conserved region of the genome. We used GERP conservation scores, which are calculated as the number of substitutions observed minus the number of substitutions expected from the species tree under a neutral model. We downloaded GERP scores (accessed from http://mendel.stanford.edu/SidowLab), which have been computed for the human reference genome version hg19. The alignment was based on 35 mammal species but did not include the domestic goat (see https://genome.ucsc.edu/cgi-bin/hgTrackUi?db=hg19&g=allHg19RS_BW for more information). Exclusion of the focal species domestic goat is recommended for the computation of conservation scores, as the inclusion of the reference genome may lead to biases [51].

348 In order to remap the GERP scores associated to hg19 positions to the domestic goat reference genome
349 positions, we used liftOver (hgdownload.cse.ucsc.edu, v.287) and the chain file downloaded from
350 hgdownload-test.cse.ucsc.edu/goldenPath/capHir1.
351
352 Third, we ascertained support for gene models annotated in the domestic goat genome with expression
353 analyses of Alpine ibex tissue samples. We included expression data from 10 organs of an Alpine ibex
354 female (see RNA-seq data section above) to assess expression levels of each gene model. Quality
355 filtering of the raw data was performed using Trimmomatic [40] v.0.36. Hisat2 [52] v.2.0.5 was used to map
356 the reads of each organ to the domestic goat reference genome. The mapping was run with option --
357 rna-strandness RF (stranded library) and supported by including a file with known splice sites (option
358 --known-splicesite-infile). The input file was produced using the script hisat2_extract_splice_sites.py
359 (part of hisat2 package) from the same gtf file as the one used for the snpEff analyis (see above). For
360 each organ, featureCounts [53] (subread-1.5.1) was used to count reads per each exon using the following
361 options: -s 2 (reverse stranded) –f (count reads at the exon level), –O (assign reads to all their
362 overlapping features), –C (excluding read pairs mapping to different chromosomes or the same
363 chromosome but on a different strand). The R package edgeR [54] was used to calculate FPKM
364 (Fragments Per Kilobase Of Exon Per Million Fragments Mapped) per each gene and organ. For variant
365 sites that were included in more than one exon, the highest FPKM value was used. We found that 16'013
366 out of 17'998 genes showed transcriptional activity of at least one exon (FPKM > 0.3). Overall 166'973
367 out of 178'504 exons showed evidence for transcription. In a total of 1928 genes, one or more exons
368 showed no evidence for transcription. Retained SNPs were found among 118'756 exons and 17'685
369 genes. Overall 611'711 out of 677'578 SNPs were located in genes with evidence for transcription.
370
371 Deleterious mutations are assumed to be overwhelmingly derived mutations. We used all ibex species
372 except Alpine and Iberian ibex as an outgroup to define the derived state. For each biallelic site, which
373 was observed in alternative state in Alpine ibex or Iberian ibex, the alternative state was defined as
374 derived if its frequency was zero in all other species (a total of 44'730 autosomal SNPs). For loci with
375 more than two alleles, the derived state was defined as unknown. For comparisons among all species,

we only used the following criteria to select SNPs (370'853 biallelic SNPs retained): transcriptional activity (FPKM > 0.3 in at least one organ), GERP > -2 and a minimal distance to the next SNP of 3bp.

Individual-based simulations with Nemo

Individual-based forward simulations were run using the software Nemo [38] v.2.3.51. A customized version of aNEMOne [55] was used to prepare input files for parameter exploration. The sim.ini file for the final set of parameters run in 100 replicates is available as Supplementary File 1. All populations relevant for the founding of the populations under study were included in the model. See Figure 6A for the simulated demography, which was modeled with the actual founder numbers (assuming a sex-ratio of 1:1), while the translocations were simplified into four phases (data from [37], DRYAD entry doi:10.5061/dryad.274b1 and [36]). The harmonic mean of the population census from the founding up to the final sampling year (2007) was used to define the population carrying capacity. Mating was assumed to be random and fecundity (mean number of offspring per female) set to five. The selection coefficients of 5000 biallelic loci subject to selection were drawn from a gamma distribution with a mean of 0.01 and a shape parameter of 0.3 resulting in $s < 1\%$ for 99.2% of all loci [56] (Figure S16). Based on empirical evidence, we assumed a negative relationship between h and s [57]. We used the exponential equation $h = \exp(-51*s)/2$ with a mean h set to 0.37 following [58]. We assumed hard selection acting at the offspring level. In addition to the 5000 loci under selection, we simulated 500 neutral loci. Recombination rates among each neutral or deleterious locus was set to 0.5. This corresponds to an unlinked state. Initial allele frequencies were set to $\mu / h * s = 0.0014$ (corresponding to the expected mean frequency at mutation-selection balance [59]). Mutation rate μ was set to 5e-05 and deleterious mutations were allowed to back-mutate at a rate of 5e-07.

A burn-in of 3000 generations was run with one population ($N = 1000$) representing the entire species allowing to reach a quasi-equilibrium. N was reduced to $N = 500$ for five generations before a brief, two generation bottleneck of $N = 80$. At generation 3007, the population recovered to $N = 1000$ and three generations later the reintroduction was started with the founding of the two zoos Interlaken Harder (ih) and Peter and Paul (pp). The founding of new populations was modeled by migration of

offspring into an empty patch.

The zoo ih (Interlaken Harder) and several populations did not survive all replicates of the simulations. Extinction rates were as follows: ih (Zoo Interlaken Harder) 84%, bo (Bire Öschinen) 3%, wh (Weisshorn) 3%, ob (Oberbauenstock) 9%, am (Alpi Marittime) 14% and pil (Pilatus) 2%. The high extinction rate of the zoo Interlaken Harder did not affect the outcome of the simulations. The extinctions were a result of the strong reduction in population size during the founding and occurred always after the founding (see also Figure S15). The extinctions of the reintroduced populations did not affect the estimates of derived allele counts but reduced sample sizes and, hence, affected the variance of estimators.

Data availability

Raw whole-genome sequencing data produced for this project was deposited at the NCBI Short Read Archive under the Accession nos. SAMN10736122–SAMN10736160 (BioProject PRJNA514886). Raw RNA sequencing data produced for this project was deposited at the NCBI Short Read Archive under the Accession nos. SAMN10839218-SAMN10839227 (BioProject PRJNA517635).

Acknowledgments

We thank the following organizations and colleagues who contributed samples to this project. Iris Biebach, the Swiss hunting authorities of the cantons of Bern, Nidwalden, Obwalden, Uri, Graubünden and Wallis; the Gran Paradiso National Park (Alice Brambilla) and the Alpi Marittime National Park (Laura Martinelli), Sebastien Regnaut and Richard Kock, Zoological Society of London, Christian Siegenthaler, Ruedi Kunz and Samer Angelone-Alasaad. We are thankful to Glauco Camenisch and Kasia Sluzek, who provided access to Alpine ibex RNAseq datasets. We thank Laurent Excoffier, Stephan Peischl, Kimberly Gilbert, Heidi Lischer, Stefan Wyder, Thomas Wicker, Alan Brelsford and Jessica Purcell for helpful advice and comments on a previous version of the manuscript. We are grateful for drawings by Nadine Coline of the Zoological Museum of Zürich. This work was supported by the University of Zurich through a University Research Priority Program "Evolution in Action" pilot project grant and the Swiss Federal Office for the Environment. DC and CG were supported by the

430 Swiss National Science Foundation (grant 31003A_173265 and 31003A_182343, respectively). This
431 study makes use of data generated by the NextGen Consortium, which was supported by grant
432 agreement number 244356 of the European Union's Seventh Framework Programme (FP7/2010-2014).
433

434 **References:**

435 1. Morton, N. E., Crow, J. F. & Muller, H. J. An estimate of the mutational damage in man
436 from data on consanguineous marriages. *PNAS* **42,** 855–863 (1956).
437 2. Frankham, R., Bradshaw, C. J. A. & Brook, B. W. Genetics in conservation management:
438 Revised recommendations for the 50/500 rules, Red List criteria and population viability
439 analyses. *Biol Conserv* **170,** 56–63 (2014).
440 3. Cruz, F., Vilà, C. & Webster, M. T. The legacy of domestication: accumulation of
441 deleterious mutations in the dog genome. *Mol Biol Evol* **25,** 2331–2336 (2008).
442 4. Renaut, S. & Rieseberg, L. H. The accumulation of deleterious mutations as a consequence
443 of domestication and improvement in sunflowers and other *compositae* crops. *Mol Biol Evol*
444 **32,** 2273–2283 (2015).
445 5. Lynch, M. Mutation and human exceptionalism: our future genetic load. *Genetics* **202,** 869–
446 875 (2016).
447 6. Marsden, C. D. *et al.* Bottlenecks and selective sweeps during domestication have increased
448 deleterious genetic variation in dogs. *PNAS* **113,** 152–157 (2016).
449 7. Laenen, B. *et al.* Demography and mating system shape the genome-wide impact of
450 purifying selection in *Arabis alpina*. *PNAS* **115,** 816–821 (2018).
451 8. Charlesworth, B. Effective population size and patterns of molecular evolution and variation.
452 *Nat Rev Genet* **10,** 195–205 (2009).
453 9. Kimura, M. Stochastic processes and distribution of gene frequencies under natural
454 selection. *Cold Spring Harb. Symp. Quant. Biol.* **20,** 33–53 (1955).
455 10. Keller, L. & Waller, D. Inbreeding effects in wild populations. *Trends Ecol Evol* **17,** 230–
456 241 (2002).
457 11. Glémin, S. How are deleterious mutations purged? Drift versus nonrandom mating.
458 *Evolution* **57,** 2678–2687 (2003).
459 12. Garcia-Dorado, A. Understanding and predicting the fitness decline of shrunk populations:
460 inbreeding, purging, mutation, and standard selection. *Genetics* **190,** 1461–1476 (2012).
461 13. Crow, J. F. Genetic loads and the cost of natural selection. in *Mathematical Topics in*
462 *Population Genetics* (ed. Kojima, K. I.) 128–177 (Springer-Verlag, 1970).
463 14. Robinson, J. A. *et al.* Genomic flatlining in the endangered island fox. *Curr Biol* **26,** 1183–
464 1189 (2016).
465 15. Kirkpatrick, M. & Jarne, P. The effects of a bottleneck on inbreeding depression and the
466 genetic load. *Am Nat* **155,** 154–167 (2000).
467 16. Bataillon, T. & Kirkpatrick, M. Inbreeding depression due to mildly deleterious mutations in
468 finite populations: size does matter. *Genet Res* **75,** 75–81 (2000).
469 17. Willi, Y., Fracassetti, M., Zoller, S. & Van Buskirk, J. Accumulation of mutational load at
470 the edges of a species range. *Mol Biol Evol* **22,** 140 (2018).
471 18. Hedrick, P. W. & Garcia-Dorado, A. Understanding inbreeding depression, purging, and
472 genetic rescue. *Trends Ecol Evol* **31,** 940–952 (2016).
473 19. Xue, Y. Mountain gorilla genomes reveal the impact of long-term population decline and
474 inbreeding. *Science* **348,** 239–242 (2015).
475 20. Rogers, R. L. & Slatkin, M. Excess of genomic defects in a woolly mammoth on Wrangel
476 island. *PLoS Genet* **13,** e1006601 (2017).
477 21. Robinson, J. A., Brown, C., Kim, B. Y., Lohmueller, K. E. & Wayne, R. K. Purging of
478 strongly deleterious mutations explains long-term persistence and absence of inbreeding
479 depression in island foxes. *Curr Biol* 1–13 (2018). doi:10.1016/j.cub.2018.08.066
480 22. Laws, R. J. & Jamieson, I. G. Is lack of evidence of inbreeding depression in a threatened
481 New Zealand robin indicative of reduced genetic load? *Animal Conservation* **14,** 47–55
482 (2011).
483 23. Kennedy, E. S., Grueber, C. E., Duncan, R. P. & Jamieson, I. G. Severe inbreeding
484 depression and no evidence of purging in an extremely inbred wild species--the Chatham
485 Island black robin. *Evolution* **68,** 987–995 (2014).
486 24. Crnokrak, P. & Barrett, S. Perspective: Purging the genetic load: A review of the
487 experimental evidence. *Evolution* **56,** 2347–2358 (2002).

25. Kalinowski, S. T., Hedrick, P. W. & Miller, P. S. Inbreeding depression in the Speke's gazelle captive breeding program. *Conserv Biol* **14,** 1375–1384 (2000).
26. Grodinsky, C. & Stuwe, M. The reintroduction of the Alpine ibex to the Swiss Alps. *Smithsonian* **18,** 68–77 (1987).
27. Biebach, I. & Keller, L. F. A strong genetic footprint of the re-introduction history of Alpine ibex (*Capra ibex ibex*). *Mol Ecol* **18,** 5046–5058 (2009).
28. Grossen, C., Biebach, I., Angelone-Alasaad, S., Keller, L. F. & Croll, D. Population genomics analyses of European ibex species show lower diversity and higher inbreeding in reintroduced populations. *Evol Appl* **11,** 123–139 (2018).
29. Reading, R. & Shank, C. *Capra sibirica:* The IUCN Red List of Threatened Species 2008. doi:10.2305/IUCN.UK.2008.RLTS.T42398A10695735.en
30. McQuillan, R. *et al.* Runs of homozygosity in European populations. *The American Journal of Human Genetics* **83,** 359–372 (2008).
31. Cooper, G. M. *et al.* Distribution and intensity of constraint in mammalian genomic sequence. *Genome Res* **15,** 901–913 (2005).
32. Couturier, M. *Le Bouquetin des Alpes*. (1962).
33. Do, R. *et al.* No evidence that selection has been less effective at removing deleterious mutations in Europeans than in Africans. *Nature* **47,** 126–131 (2015).
34. Terrier, G. & Rossi, P. Le bouquetin (*Capra ibex ibex*) dans les alpes maritimes franco-italiennes: occupation de l'éspace, clonisation et régulation naturelles. *Traveaux Scientifiques du Parc National de la Vanoise* **XVIII,** 271–288 (1994).
35. Maudet, C. *et al.* Microsatellite DNA and recent statistical methods in wildlife conservation management: applications in Alpine ibex *Capra ibex (ibex)*. *Mol Ecol* **11,** 421–436 (2002).
36. Biebach, I. & Keller, L. F. Inbreeding in reintroduced populations: the effects of early reintroduction history and contemporary processes. *Conserv Genet* **11,** 527–538 (2010).
37. Aeschbacher, S., Futschik, A. & Beaumont, M. A. Approximate Bayesian computation for modular inference problems with many parameters: the example of migration rates. *Mol Ecol* **22,** 987–1002 (2013).
38. Guillaume, F. & Rougemont, J. Nemo: an evolutionary and population genetics programming framework. *Bioinformatics* **22,** 2556–2557 (2006).
39. Lynch, M., Conery, J. & Burger, R. Mutation accumulation and the extinction of small populations. *Am Nat* **146,** 489–518 (1995).
40. Bolger, A. M., Lohse, M. & Usadel, B. Trimmomatic: a flexible trimmer for Illumina sequence data. *Bioinformatics* **30,** 2114–2120 (2014).
41. Dong, Y. *et al.* Sequencing and automated whole-genome optical mapping of the genome of a domestic goat (*Capra hircus*). *Nat Biotechnol* **31,** 135–141 (2012).
42. Langmead, B. & Salzberg, S. L. Fast gapped-read alignment with Bowtie 2. *Nature Methods* **9,** 357–359 (2012).
43. McKenna, A. *et al.* The Genome Analysis Toolkit: a MapReduce framework for analyzing next-generation DNA sequencing data. *Genome Res* **20,** 1297–1303 (2010).
44. DePristo, M. A. *et al.* A framework for variation discovery and genotyping using next-generation DNA sequencing data. *Nat Genet* **43,** 491–498 (2011).
45. Garrison, E. FreeBayes source repository. Available at: https://github.com/ekg/freebayes. (Accessed: 14 November 2018)
46. Danecek, P. *et al.* The variant call format and VCFtools. *Bioinformatics* **27,** 2156–2158 (2011).
47. Narasimhan, V. *et al.* BCFtools/RoH: a hidden Markov model approach for detecting autozygosity from next-generation sequencing data. *Bioinformatics* **32,** 1749–1751 (2016).
48. Dumont, B. L.Payseur, Bret A. Evolution of the genomic rate of recombination in mammals. *Evolution* **62,** 276–294 (2008).
49. Cingolani, P. *et al.* A program for annotating and predicting the effects of single nucleotide polymorphisms, SnpEff: SNPs in the genome of Drosophila melanogaster strain w(1118); iso-2; iso-3. *fly* **6,** 80–92 (2012).
50. Jones, P. *et al.* InterProScan 5: genome-scale protein function classification. *Bioinformatics* **30,** 1236–1240 (2014).

51. Fu, W., Gittelman, R. M., Bamshad, M. J. & Akey, J. M. Characteristics of neutral and deleterious protein-coding variationamong individuals and populations. *Am J Hum Genet* **95,** 421–436 (2014).
52. Kim, D., Langmead, B. & Salzberg, S. L. HISAT: a fast spliced aligner with low memory requirements. *Nature Methods* **12,** 357–360 (2015).
53. Liao, Y., Smyth, G. K. & Shi, W. featureCounts: an efficient general purpose program for assigning sequence reads to genomic features. *Bioinformatics* **30,** 923–930 (2014).
54. Robinson, M. D., McCarthy, D. J., Bioinformatics, G. S.2010. edgeR: a Bioconductor package for differential expression analysis of digital gene expression data. *academic.oup.com*
55. kjgilbert/aNEMOne. (2017).
56. Keightley, P. D. The distribution of mutation effects on viability in Drosophila melanogaster. *Genetics* **138,** 1315–1322 (1994).
57. Agrawal, A. F. & Whitlock, M. C. Inferences about the distribution of dominance drawn from yeast gene knockout data. *Genetics* **187,** 553–566 (2011).
58. Gilbert, K. J. *et al.* Local Adaptation Interacts with Expansion Load during Range Expansion: Maladaptation Reduces Expansion Load. *Am Nat* **189,** 368–380 (2017).
59. Crow, J. F. & Kimura, M. *An Introduction to Population Genetics Theory*. (New Jersey: Blackburn Press, 1970).
60. IUCN 2018. *httpwww.iucnredlist.org* Available at: (Accessed: 10 November 2018)

Figure legends

Figure 1: Characterization of sampled ibex species. A) Geographical distribution and IUCN conservation status of ibex and wild goat species (LC: Least concern, V: Vulnerable, NT: Near threatened [60]). Sample sizes: *C. ibex*: N=29, *C. pyrenaica*: N=4, *C. aegagrus*: N=6, *C. sibirica*: N=2, *C. falconeri*: N=1, *C. nubiana*: N=2. B) Maximum likelihood phylogenetic analyses, C) nucleotide diversity, D) proportion of the genome with runs of homozygosity (ROH) longer than 2.5 Mb and E) percentage of polymorphic sites within species that segregate highly deleterious mutations.

Figure 2: Segregating deleterious mutations in Alpine and Iberian ibex. A) Population sampling locations of Iberian ibex (left, grey circles) and Alpine ibex (right, colored circles). Each filled circle represents a population. Circles with a black outline indicate the first three reintroduced populations in Switzerland that were used for all subsequent population reintroductions of Alpine ibex. Colors associate founder and descendant populations (see also Figure 3A). Site frequency spectra for neutral (modifier), mildly (moderate impact) and highly deleterious (high impact) mutations for (B) Iberian

582 and (C) Alpine ibex. D) *Rxy* analysis contrasting Iberian with Alpine ibex across the spectrum of impact
583 categories. *Rxy* < 1 indicates a relative frequency deficit of the corresponding category in Alpine ibex
584 compared to Iberian ibex. E) Individual homozygote counts per impact category for Iberian (light green)
585 and Alpine ibex (dark green).
586
587 **Figure 3: Population genomic consequences of Alpine ibex recolonization**. A) Schematic showing
588 the recolonization history and population pedigree of Alpine ibex. Locations include also zoos and the
589 population Pilatus (pi), which was not sampled for this study but is known to have contributed to the
590 population Oberbauenstock (ob). am: Alpi Marittime, gp: Gran Paradiso; ih: Zoo Interlaken Harder; al:
591 Albris; bo: Bire Öschinen; br: Brienzer Rothorn; ob: Oberbauenstock; pl: Pleureur; rh: Rheinwald; wh:
592 Weisshorn; pi: Pilatus; pp: Wildpark Peter and Paul. The grey circle represents a population that was
593 founded from more than one population. Figure elements were modified from Biebach and Keller
594 (2009) with permission. B) Principal component analysis of all Alpine ibex individuals included in the
595 study. C) Nucleotide diversity per population. D) Proportion of the genome within runs of
596 homozygosity (ROH) longer than 2.5 Mb. E) *Rxy* analysis contrasting the strongly bottlenecked Alpi
597 Marittime population with all other Alpine ibex populations across the spectrum of impact categories.
598 *Rxy* < 1 indicates a relative frequency deficit of the corresponding category in the Alpi Marittime
599 population. Circles with a black outline indicate the first three reintroduced populations in Switzerland
600 that were used for all subsequent population reintroductions of Alpine ibex. Colors associate founder
601 and descendant populations.
602
603 **Figure 4: Impact of recolonization on the mutation load per individual.** (A) Homozygote counts
604 and (B) allele counts per individual for each Alpine ibex population. The schematic between A and B
605 indicates the harmonic mean of the census size of each population, which is inversely correlated with
606 the strength of drift. *) Estimated numbers. Colors associate founder and descendant populations (see
607 also Figure 3A).
608

609 **Figure 5: Homology-based inference of the impact of highly deleterious mutations.** The
610 localization of protein family (PFAM) domains are highlighted in dark. Red dots indicate the relative
611 position of a highly deleterious mutation segregating in Alpine ibex. The frequencies of highly
612 deleterious mutations are summarized for Iberian ibex and three subsets of Alpine ibex. The
613 demographic history is shown with a schematic.
614
615 **Figure 6: Individual-based forward simulations recapitulating the reintroduction history of**
616 **Alpine ibex**. A) Demographic model used for the individual-based simulations. The model was
617 parametrized using census data and historical records (see methods). Bold numbers represent the
618 carrying capacities defined as the harmonic mean of the census size. Numbers not in bold represent
619 the number of individuals released to found each population. If a population was established from two
620 source populations, the individual numbers are separated by commas. *) Upwards adjusted harmonic
621 means of the census size (historical records were ih = 16 and pp = 20). The adjustment was necessary
622 to prevent extinction of zoo populations. **) Census numbers were estimated based on historical
623 records of the population but no long- term data census data was available. B) Relative frequency
624 comparison (*Rxy*) of Alpine ibex just before and after the species bottleneck and recolonization. C)
625 *Rxy* analysis contrasting the strongly bottlenecked Alpi Marittime population with all other Alpine
626 ibex populations across the spectrum of impact categories. D) Individual homozygote counts per
627 impact category. Boxplots summarized 100 population means across simulation replicates. Colors
628 associate founder and descendant populations (see also Figure 3A).

Figure 1

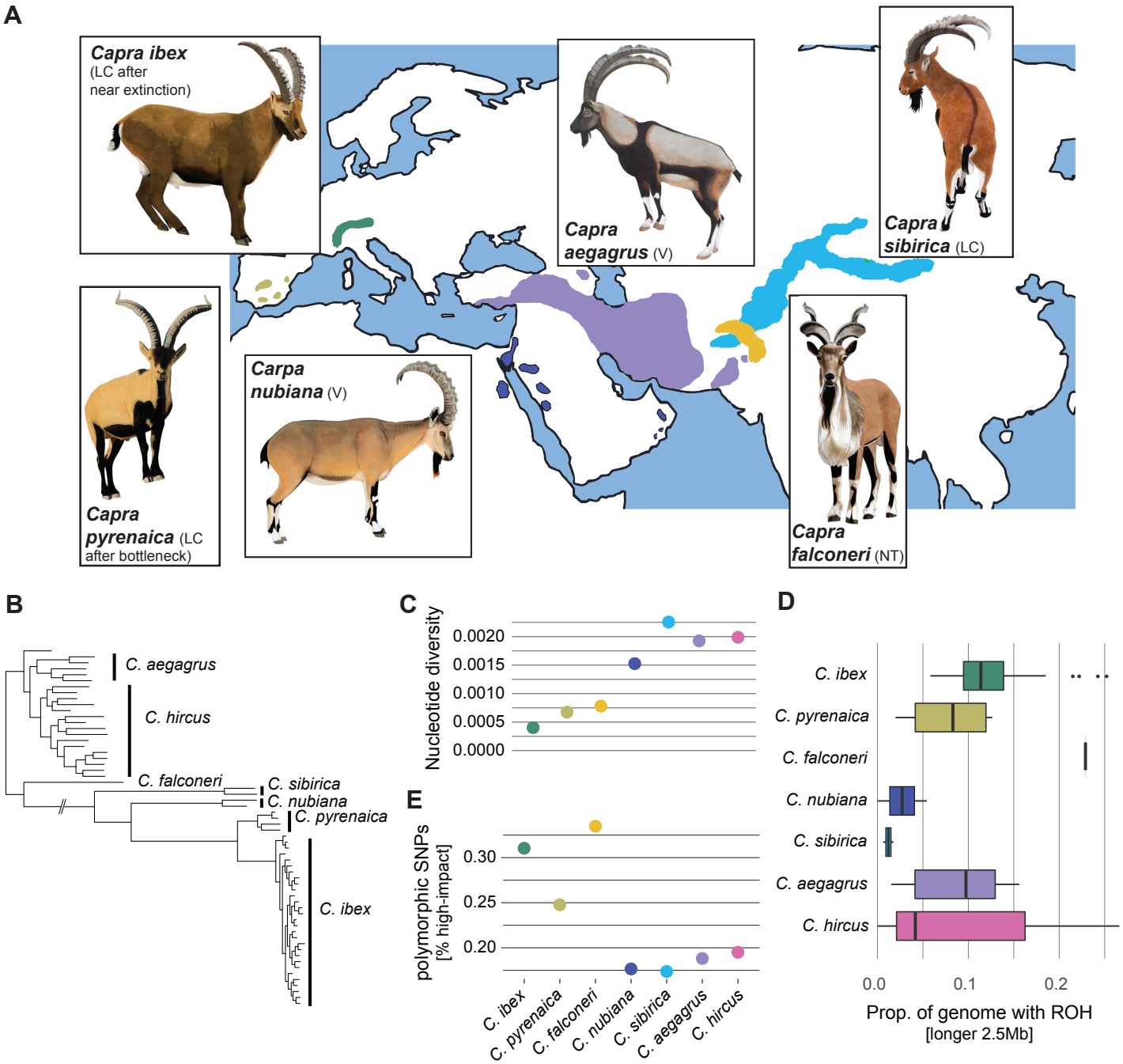

Figure 2

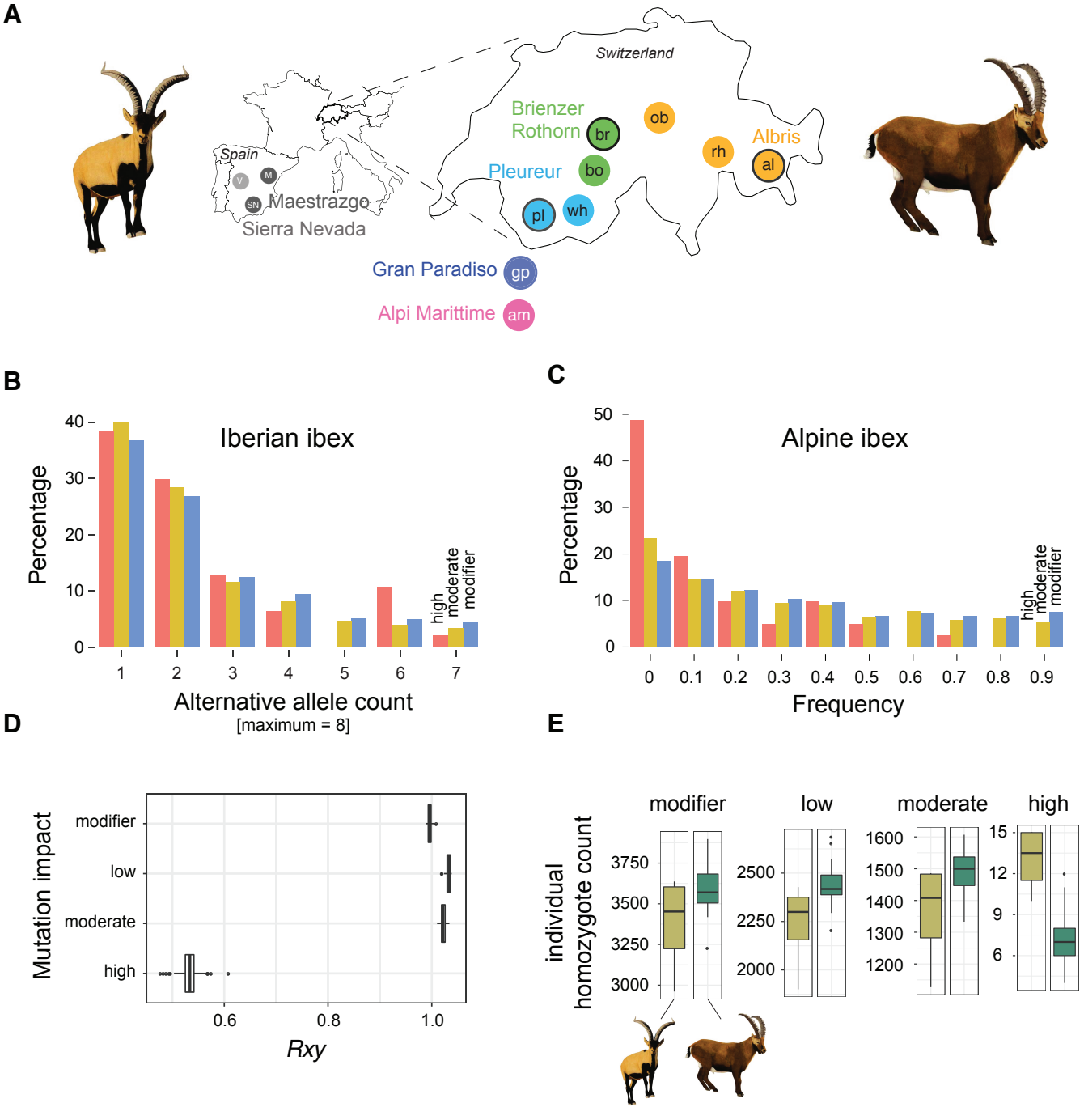

Figure 3